DTIC FILE COPY

Limnol. Oceanogr., 34(8), 1989, 1673–1693
© 1989, by the American Society of Limnology and Oceanography, Inc

AD-A226 023

Estimation of a photon budget for the upper ocean in the Sargasso Sea

R. C. Smith
Department of Geography, University of California, Santa Barbara 93106

J. Marra
Lamont-Doherty Geological Observatory of Columbia University, Palisades, N.Y. 10964

M. J. Perry
School of Oceanography, University of Washington, Seattle 98195

K. S. Baker
Scripps Institution of Oceanography, A-018, UCSD, La Jolla, California 92093

E. Swift
Graduate School of Oceanography, University of Rhode Island, Kingston 02881

E. Buskey
Marine Science Institute, University of Texas at Austin, Port Aransas 78373

D. A. Kiefer
Department of Biological Sciences, University of Southern California, Los Angeles 90089-0371

DTIC
ELECTE
AUG 27 1990
S B D

Abstract

A photon budget based on the quanta absorbed and subsequent biological utilization is computed for a site in the northwestern Sargasso Sea in spring. The budget includes sources, transitions, and sinks for photosynthetically available radiation (PAR). The attentuation of PAR is partitioned into separate components and the loss caused by each component is estimated as a function of depth in the upper 100 m. The major sources of attenuation to PAR include seawater (35–76%), total particulate material (20–65%), and dissolved organic material (0–13%). The total particulate material attentuation could be partitioned into attenuation of phytoplankton (12–39%) and of detrital material (8–27%). Although the greatest fraction of photons is absorbed by water, all the variability within the budget is caused by biological processes. Source terms include bioluminescence and chlorophyll *a* fluorescence, which are orders of magnitude less than radiant energy attenuation, but they are detectable and biologically significant. This photon budget is an estimate, on a quantum basis, of how radiant energy is absorbed and how various fractions are converted to chemical energy or lost to nonphotosynthetic processes. The budget serves to focus on sources, transitions, and sinks of photons and elucidate the mechanisms linking biological processes and ocean optical properties; to identify the major absorbers in the ocean and quantify their relative influence; to demonstrate an accounting with respect to the penetration of radiant energy into natural waters and point to major assumptions and uncertainties in our current estimate; and to establish a perspective that can serve as a basis for the predictive linkage of optical variability and bioluminescence.

Acknowledgments

Recognition and thanks are given to R. Bidigare for pigment analysis and critique of the manuscript, to D. Siegel for discussions, to W. S. Chamberlin for laboratory work, and to C. Johnson for technical assistance.

The work was supported by the Oceanic Biology and Ocean Optics Programs of the Office of Naval Research under the following contracts: N00014-84-C-0382 (R.C.S., K.S.B.); N00014-84-C-0132-IIA (J.M.), N00014-84-C-0111 (M.J.P.), N00014-81-C-0062 (E.S., E.B.), N00014-84-K-0363 (D.K.).

Biowatt Contribution 26.

Optical properties of the upper ocean and the penetration of solar radiation are of primary importance in oceanography. Optical properties are determined by the dissolved and suspended inorganic and biotic constituents in the water. By harvesting radiant energy, plants modify both the optical properties and the radiant energy field for other organisms in the water column. Penetration of solar radiation also affects zooplankton

DISTRIBUTION STATEMENT A
Approved for public release;
Distribution Unlimited

90 08 24 041

behavior and has direct influence on thermal structure in the upper ocean. In this work we present a budget for in-water radiant energy [for photosynthetically available radiation (PAR), 400–700 nm] for the water column to focus on important sources and sinks of radiant energy and the interrelations between biological processes and ocean optical properties, quantify the relative influence of major absorbers and scatterers, demonstrate an accounting of the penetration of radiant energy into natural waters, outline the major assumptions and uncertainties in this estimate, and identify important biological and environmental variables as well as their associated errors and uncertainties. The data used here are from Biowatt station 19 at 35°N, 70°W. The station was occupied in April 1985. Background information on the Biowatt program can be found elsewhere (Marra and Hartwig 1984).

The utilization of solar radiation by phytoplankton has been discussed frequently and summarized by Talling (1982) and Kirk (1983). From this early work it is known that the proportion of absorbed PAR captured by phytoplankton is highly variable, ranging from a few percent in oligotrophic lakes and open ocean areas to as high as 20–40% in highly productive lakes and ocean coastal waters. It is also known that the patterns of photosynthetic utilization are a complex function of biological processes and optical properties which vary in space and time. The multidisciplinary work reported here is distinguished by detailed spectral irradiance data as a function of depth and time, complete pigment information using high performance liquid chromatographic (HPLC) analysis, spectral absorption measurements for particulate and detrital material, relatively "clean" in situ ^{14}C assimilation experiments to estimate phytoplankton productivity, contemporaneous information on bioluminescent organisms, and full spectral computation for all major parameters in the budget. We estimate the sinks and the sources of photons (400–700 nm) as a function of depth (generally to 100 m). We chose the total diffuse attenuation coefficient for downward irradiance, $K_d(z, \lambda)$ to characterize the bio-optical state of ocean water (Smith and Baker 1978; Baker and Smith 1982). Our main reason for this choice is that $K_d(z, \lambda)$ is the property directly derivable from spectral irradiance measurements and the property, when known, that allows the spectral irradiance at depth, $E_d(z, \lambda)$, to be calculated from the measurement of spectral irradiance just below the air–water interface, $E_d(0^-, \lambda)$. Even when the inherent optical properties of absorption, $a(z, \lambda)$, and scattering, $b(z, \lambda)$, for a water column are fully known, the apparent optical property $K_d(z, \lambda)$ must be derived in order to compute the attenuation of radiant energy as a function of depth.

For the photon budget, we make use of the quasi-inherent optical properties of the attenuation coefficient (Højerslev 1974; Smith and Baker 1978; Kirk 1983) that can be partitioned into separate components. Total incoming photons are partitioned first into those photons attenuated by water, particulate material, and dissolved organic matter. For these clear ocean waters it is assumed that the absorption due to inorganic particles is negligible. Those photons not converted by photochemical processes, such as the attenuation by water, are lost to heat. The subset of photons attenuated by particles is further partitioned into photons used photochemically (to reduce carbon for energy storage in organic matter) and those lost by detrital absorption. These computations are relatively precise. For completeness in assessing the biological contributions to optical variability, we also make simple estimates of biologically linked photons that are emitted as fluorescence or bioluminescence. Other sources of transpectral scattering (e.g. Raman and Brillouin scattering) are ignored. Fluorescence, linked to biological processes through the opening and closing of reaction centers, occurs on a time scale appropriate to the electron transport through the photosystem. Bioluminescence is a biologically controlled process, modified to some degree by external stimulation, which occurs on time scales that are less appropriate for a strict photon accounting. We include a discussion of bioluminescence in order to account for biological processes that may influence the external light field and to search for possible predictive link-

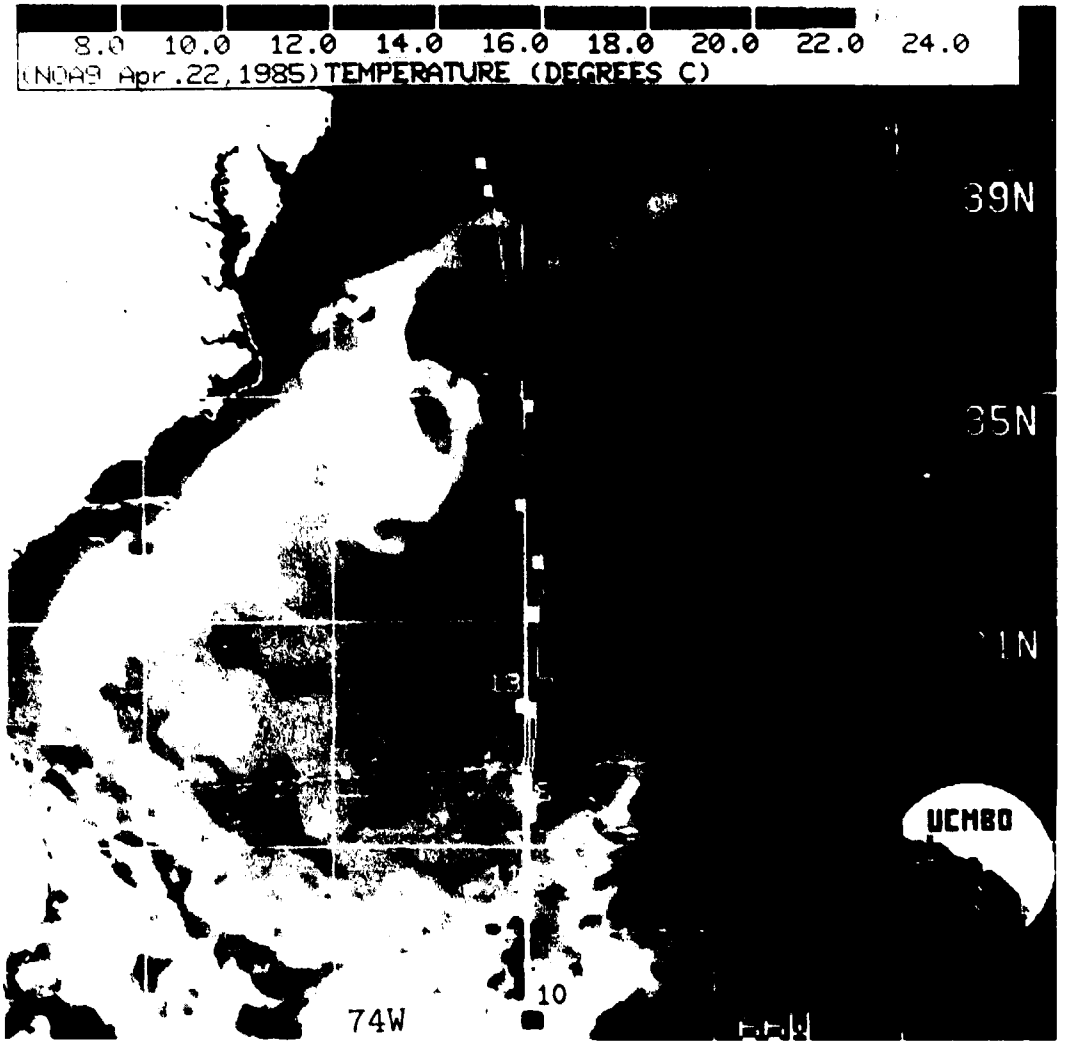

Fig. 1. Advanced high resolution radiometer (AVHRR) image of sea surface temperature (SST) from 22 April 1985. Dark regions correspond to regions of cooler SST. The ship track and station locations are shown.

ages between optical variability and bioluminescence. Thus, the photon budget is an assessment—on a quantum basis—of how radiant energy is absorbed, of the fraction converted into chemical energy, and of the fraction associated with the biological emission of photons. The goal is a quantum-based photon budget (rather than an energy budget) based on absorption and subsequent biological utilization or re-emission of quanta and improving our understanding of the biological relationships that produce a specific set of optical conditions.

Methods

General—The Biowatt I cruise took place 2–28 April 1985 aboard RV *Knorr* and consisted of a transect to 35°N, 70°W where a 5-d time-series station was taken (station 4), a north–south transect from 35° to 24°N (stations 4–10) including a 4-d time series at the southernmost station, transect back south to north (stations 11 through 18), and reoccupation of the northernmost transect station (station 19) for a repeat time series (Fig. 1). For station 19 the ship was stationed for 7 d (19–25 April) at 35°N, 70°W—

odes
or
Dist Special
DTIC COPY INSPECTED
A-1 21

a location east of the Gulf Stream and about half way between Cape Hatteras and Bermuda.

Shipboard observations and satellite imagery from the time of the cruise indicate that the first occupation of 35°N, 70°W (station 4) was during a diatom bloom and that the subsequent occupation (station 19) was characterized by a postbloom phytoplankton community (Bidigare et al. 1989). Siegel et al. (in prep.) have shown that the evolution of the subtropical mode (18°C) water mass is the primary factor controlling the spatial distribution and temporal evolution of the phytoplankton community and hence optical properties in the northern Sargasso Sea (31°–35°N). They hypothesize that the springtime near-surface restratification initiates a diatom-dominated phytoplankton bloom. As the diatom bloom decays, it is succeeded by other algal classes characterized by relatively lower pigment and smaller particle volume concentrations and sizes. In particular, the phytoplankton assemblage for this photon budget was postdiatom bloom and comprised of small cells (5 μm and less) with a high cyanobacterial fraction (Iturriaga and Marra 1988). Thus, the work reported here may be representative of summer central gyre areas of the open oceans.

The data collected during a 3-d period (20–22 April 1985) were chosen for this photon budget because of the relative hydrographic stability shown by time-series data. Given the wide variety of measurements involved, not all parameters could be observed simultaneously. The data on particles and production were collected from casts taken at dawn on 22 April (station-cast 19.50), but submarine irradiance was measured throughout the day (station-casts 19.49–19.58) with 19.51 being made <1 h after 19.50. Bioluminescence observations measured at night on 20–21 April are used in constructing a budget for 22 April.

Shipboard measurements—Water samples were taken and hydrographic measurements were performed with a conductivity-temperature-depth (CTD) profiler having a 12-bottle rosette equipped with 8-liter Niskin bottlers and with the bio-optical profiling system (BOPS) (Smith et al. 1984) having a 10-bottle rosette equipped with 1.7-liter Niskin bottles. The CTD and BOPS included sensors to determine depth, temperature, and conductivity along with in situ fluorescence using a Sea Martec and a Q-Instrument, respectively. Continuous optical profiles were made using BOPS—an instrument package with an above-water deck unit measuring downwelling spectral irradiance and an underwater unit with upward- and downward-looking spectral irradiance units as well as a beam transmissometer measuring at 665 nm (Bartz et al. 1978). Windspeed and total downwelling irradiance (285–2,800 nm) were recorded at 1-min intervals from atop the forward superstructure of the ship.

Chlorophyll *a* and pheopigments were routinely determined by the method of Smith et al. (1981) with a Turner model 111 fluorometer calibrated spectrophotometrically (Jeffrey and Humphrey 1975) with pure Chl *a* (Sigma Chemical Co.). High performance liquid chromatographic (HPLC) pigment analyses were performed as detailed by Bidigare et al. (1989). Particulate absorption measurements were made following the procedure of Mitchell and Kiefer (1988) and provided a measure of the spectral absorption caused by living and nonliving particles. For estimation of quantum yield, the phytoplankton component was resolved with an end-member reconstruction technique based on the absorption spectra of pure phytoplankton (Cleveland et al. 1989). Particulate organic carbon and nitrogen were determined with a Perkin-Elmer 240D elemental analyzer using 1-liter samples that had been filtered onto precombusted Whatman GF/F filters.

Primary production was determined with the ^{14}C technique. All ^{14}C assimilation experiments were incubated in situ. As much care as possible was taken to avoid contamination of the samples during sampling and incubation, although a completely clean protocol (Fitzwater et al. 1982) could not be attained. Samples were incubated in clean, 250-ml polycarbonate bottles. The ^{14}C stock was cleansed of trace metals and kept in a Teflon bottle. Samples were filtered onto Millipore HA filters, treated with weak HCl

and counted by liquid scintillation spectroscopy. Details of the method and the *P-I* incubators can be found elsewhere (Talbot et al. 1985). Quantum yield was calculated from the light-limited slope of the *P-I* curve and the particulate absorption coefficients that were corrected for detritus.

Bioluminescence measurements—Vertically stratified zooplankton samples were collected with a multiple opening/closing net environmental sensing system (MOCNESS) with a 1-m^2 opening, and nets with 153-μm mesh (Wiebe et al. 1976, 1985). This net system allows for the collection of nine sequential zooplankton samples along with concurrent environmental information (depth, temperature, conductivity) and sampling data (flow counts, net angle). The first net sampled from the surface to a depth of 800 m. The remaining eight nets were tripped at depths of 800, 600, 500, 400, 300, 200, 100, and 50 m. Each net filtered from 250 to 700 m^3 of seawater. For station 4, the cod-end bucket had meshes of 250 μm; at stations 10 and 19, the buckets had 153-μm mesh, which matched the mesh of the nets. Samples were preserved in 4% (buffered) Formalin.

The biomass of the zooplankton samples was estimated by measuring displacement volumes after first removing large gelatinous zooplankton and fish (Beers 1976). The abundances of major groups of bioluminescent organisms (fish, decapods, polychaetes, copepods, ostracods, larvaceans, and euphausiids) were estimated by counting aliquots taken from the MOCNESS samples. The numbers include several developmental stages for each group. The copepod numbers include adults and all copepodite stages, and the euphausiid numbers include adults and all furcilia stages. The copepod numbers include only species of *Pleuromamma, Lucicutia,* and *Heterorhabdis,* all known to be bioluminescent (Herring 1978). Almost all euphausiid species are capable of bioluminescence. For all other groups total numbers are reported.

Stimulated bioluminescence—Stimulable bioluminescence was measured with a bathyphotometer (Swift et al. 1985) at 10- or 20-m depth intervals for 5 min at each depth. At the sampled depths, water was pumped through the bathyphotometer sampling chamber at a rate of 15 liters min^{-1}. There was a 15-cm spacer between the photomultiplier tube and the sampling chamber where the organisms were stimulated. The spacer makes the intensity of bioluminescence less dependent on the positions of the organisms passing through the chamber.

The optical efficiency of the bathyphotometer was determined before and after the cruise as described by Swift et al. (1985) with cultures of the dinoflagellate *Pyrocystis lunula* to fill the detection chamber. At sea, the efficiency of the bathyphotometer for measuring total stimulable bioluminescence was determined using *Pyrocystis noctiluca*. The at-sea efficiency agreed to within 10% of the laboratory value. The bioluminescence potential per unit volume of the water was estimated following the assumptions outlined by Swift et al. (1985).

Irradiance calculations—The data from the bio-optical profiling system were used to obtain estimates of quanta at depth throughout the day. The reduction of optical data collected by BOPS has been described by Smith and Baker (1984, 1986) and Siegel et al. (in prep.). It is necessary to extrapolate from a limited number of BOPS casts during the day to the entire daylight period, while knowing the above-water total irradiance that was measured continuously. This is an important calculation to attend to in detail since both above-water and submarine irradiances change dramatically over a time scale of hours. We emphasize that although the final discussions are in terms of broadband PAR irradiance, all computations have been carried out as a function of depth and wavelength so that full spectral variability as a function of depth and time have been retained. In addition, we clearly distinguish between PAR irradiance given in energy units, E_{PAR}(W m^{-2}), and PAR quantum irradiance, E_{qPAR}(quanta m^{-2} s^{-1}).

The downwelling spectral irradiance data for each BOPS cast, $E_d(z, \lambda)$, were corrected for atmospheric variability using on-deck spectral irradiance data, smoothed to eliminate fluctuations caused by surface wave action (Smith and Baker 1984), and cor-

Significant symbols

α	Initial slope of P-I curve, mg C (mg Chl a)$^{-1}$ h^{-1} (μmoles photons m^{-2} s^{-1})$^{-1}$
$a(z, \lambda)$	Volume absorption coefficient, m^{-1}
$a_d^*(z, \lambda)$	Diffuse absorption coefficient for downwelling irradiance, m^{-1}
$a_{dc}(\lambda)$, $a_p(\lambda)$, $a_{p'}(\lambda)$	Absorption coefficient due to detrital and particulate material and to phytoplankton, m^{-1}
$a_{p'}(z)$	Absorption coefficient due to particulate matter weighted by spectral irradiance at each depth, m^{-1}
$b(z, \lambda)$	Volume scattering coefficient, m^{-1}
$b_{bd}^*(z, \lambda)$, $b_{bu}^*(z, \lambda)$	Diffuse backscattering coefficient for downwelling and upwelling irradiance, m^{-1}
$b_{bdp}^*(z)$	Diffuse backscattering coefficient for downwelling irradiance due to particles, m^{-1}
Bl(z)	Bioluminescence, photons m^{-2} s^{-1}
dP/dV	Radiant PAR absorbed per unit volume, quanta m^{-3} s^{-1}
$E_d(z, \lambda)$, $E_u(z, \lambda)$	Downwelling and upwelling spectral irradiance at depth, W m^{-2} nm^{-1}
$E_{PAR}(z)$	Photosynthetically available radiation (400–700 nm), energy units, W m^{-2}
$E_{qPAR}(z)$	Photosynthetically available radiation (400–700 nm), quantum units, quanta m^{-2} s^{-1}
$E_{tot}(z)$	Total irradiance (285–2,800 nm), W m^{-2}
Fl(z)	Fluorescence, photons m^{-2} s^{-1}
I_k	P-I saturation parameter, μmoles photons m^{-2}s^{-1}
$K_d(z, \lambda)$	Total diffuse attenuation coefficient for downward irradiance, m^{-1}
$K_{dc}(z, \lambda)$, $K_p(z, \lambda)$, $K_{p'}(z, \lambda)$	Diffuse attenuation coefficient for downward irradiance due to detrital and particulate material and to phytoplankton, m^{-1}
K_{qPAR}	Total diffuse attenuation coefficient for PAR (400–700 nm), m^{-1}
$K_w(z, \lambda)$, $K_y(z, \lambda)$	Diffuse attenuation coefficient for downward irradiance due to clear seawater and to dissolved organic matter, m^{-1}
P	Photosynthesis, mg C (mg Chl a)$^{-1}$ h^{-1}
PSR, PUR	Photosynthetically stored or used radiation, moles photons m^{-3} d^{-1}
$R(z, \lambda)$	Irradiance ratio ($=E_u/E_d$)
$\bar{\mu}_d(z, \lambda)$	Average cosine for downwelling irradiance
z	Depth, m
λ	Wavelength, nm

rected for presence of the ship (Smith and Baker 1986). The spectral attentuation coefficients for a particular cast are determined from

$$K_d(z, \lambda) = -\frac{1}{z_2 - z_1} \times \ln\frac{E_d(z_1, \lambda)}{E_d(z_2, \lambda)} \quad (1)$$

where $z = (z_1 + z_2)/2$ (units given in list of symbols).

Continuous estimates of above-water irradiance $E_{tot}(0^+)$ (285–2,800 nm) were obtained with an Eppley pyranometer. These continuous data were divided into 1-h periods consistent with the vertical profiling sampling period. Photosynthetically available radiation, $E_{PAR}(0^+)$, was calculated from the pyranometer data using (Baker and Frouin 1987)

$$E_{PAR}(0^+, t) = 0.53 \times E_{tot}(0^+, t) \quad (2)$$

where t represents an hourly average. The factor 0.53 in Eq. 2 is accurate to within 3% for sun zenith angles $<70°$. Since the contribution to total daily irradiance is small at either sunrise or sunset, the error introduced by a constant factor between E_{PAR} and E_{tot} is insignificant for our purposes. These above-surface broadband estimates of E_{PAR} agreed well with periodic measurements of $E_d(0^+, \lambda)$, and integrated to give E_{PAR}, made with a spectroradiometer.

We used $E_d(0^+, \lambda, \text{noon})$ to give an estimate of $E_{PAR}(0^+, \text{noon})$ through integration over wavelength. Since the spectral shape remains relatively constant throughout the day except near low sun angles, a continuous estimate of above-water spectral irradiance at any time of day, $E_d(0^+, \lambda, t)$, can be approximated by adopting a normalization against noon,

$$E_d(0^+, \lambda, t) = E_d(0^+, \lambda, \text{noon}) \times \frac{E_{PAR}(0^+, t)}{E_{PAR}(0^+, \text{noon})}. \quad (3)$$

Although there is a measurable spectral shift near low sun angles, the contribution to daily E_{qPAR} at this time of day is small. $E_d(0^+, \lambda, t)$ is propagated through the air–water interface to give the irradiance just below the surface, $E_d(0^-, \lambda, t)$ (Smith and Baker 1986). With $E_d(0^-, \lambda, t)$ and $K_d(z, \lambda)$, $E_d(z, \lambda, t)$ is calculated at designated time intervals.

$E_{qPAR}(z, t)$—PAR in terms of quanta—is calculated from the downwelling spectral irradiance

$$E_{qPAR}(z, t) = 1/hc \times \int E_d(z, \lambda, t)\lambda \, d\lambda \quad (4)$$

where the wavelength interval is taken from 400–700 nm. Daily $E_{qPAR}(z)$ is found through integration over time.

Partial vertical attenuation coefficients—Central to the budget is the concept that the vertical attenuation coefficient for downward irradiance can be partitioned into a set of partial vertical attenuation coefficients, each corresponding to a different set of dissolved and/or suspended constituents within the medium. Preisendorfer (1961, 1976), from radiative transfer theory, derived the relationship between the diffuse attenuation coefficient, $K_d(z, \lambda)$, the diffuse absorption, $a_d^*(z, \lambda)$, and the diffuse backscattering coefficient, $b_{bd}^*(z, \lambda)$,

$$K_d(z, \lambda) = a_d^*(z, \lambda) + b_{bd}^*(z, \lambda) - b_{bu}^*(z, \lambda)R(z, \lambda) \quad (5)$$

where $b_{bd}^*(z, \lambda)$ is the diffuse backscattering coefficient for the downwelling stream of photons, $b_{bu}^*(z, \lambda)$ the diffuse backscattering coefficient for the upwelling stream, and $R(z, \lambda)$ the irradiance reflectance. In this notation an asterisk denotes an optical property determined for a diffuse (e.g. a natural) light field.

The above relationship shows that the attenuation of downward irradiance is the result of three processes represented by the three terms on the right-hand side of Eq. 5. First, the diffuse absorption coefficient of the downwelling stream,

$$a_d^*(z, \lambda) = a(z, \lambda)/\bar{\mu}_d(z, \lambda) \quad (6)$$

where $a(z, \lambda)$ is the volume absorption coefficient as measured with collimated light and $\bar{\mu}_d(z, \lambda)$ the average cosine for downwelling irradiance; second, downwelling photons removed by upward scattering; and third, an opposing process of downward-scattered photons from the upwelling stream.

The reflectance at any depth, $R(z, \lambda)$, is calculated from the ratio of upwelling to downwelling irradiance, or

$$R(z, \lambda) = E_u(z, \lambda)/E_d(z, \lambda) \quad (7)$$

where the subscripts u and d refer to upwelling and downwelling irradiance. Kirk (1981) showed that at low values of scattering to absorption (up to b/a ratios of about 5, as is true for the open ocean) the attenuation is almost entirely caused by absorption. In such cases the attenuation can be approximated:

$$K_d(z, \lambda) = a(z, \lambda)/\bar{\mu}_d(z, \lambda) + b_{bd}^*(z, \lambda). \quad (8)$$

Given this approximation along with the knowledge that an inherent optical property can be partitioned into components, it follows that the partitioning of the diffuse attenuation coefficient of irradiance into separate components is a good approximation for our work in the Sargasso Sea. The approximation becomes increasingly inaccurate as the ratio of scattering to absorption becomes large.

Thus, in spite of its status as an apparent optical property, the downwelling diffuse attenuation coefficient for irradiance can be partitioned into a set of partial vertical attenuation coefficients, each corresponding to a different component of the medium. The separate components of $K_d(z, \lambda)$ are strictly linear functions of the concentrations of the various components only for small increments in concentrations (Kirk 1983). We make use of this approximation to partition incoming photons,

$$K_d(z, \lambda) = K_w(z, \lambda) + K_p(z, \lambda) + K_y(z, \lambda), \quad (9)$$

into those attenuated by water (K_w), by particulate material (K_p), and by dissolved organic matter (K_y).

When appropriate integration over wavelength is carried out,

$$K_{PAR}(z) = K_w(z) + K_p(z) + K_y(z) \quad (10)$$

where the total diffuse attenuation coefficient for PAR, $K_{PAR}(z)$, is computed from

$$K_{PAR}(z) = -\frac{1}{z_2 - z_1} \times \ln\frac{E_{qPAR}(z_1, t)}{E_{qPAR}(z_2, t)}. \quad (11)$$

Results

Local environment—The days during the period of our study were mostly sunny with calm seas (Fig. 2). Photosynthetically available radiation averaged about 50 moles photons $m^{-2} d^{-1}$ during 20–22 April. Windspeed averaged 6–7 m s^{-1} and showed an

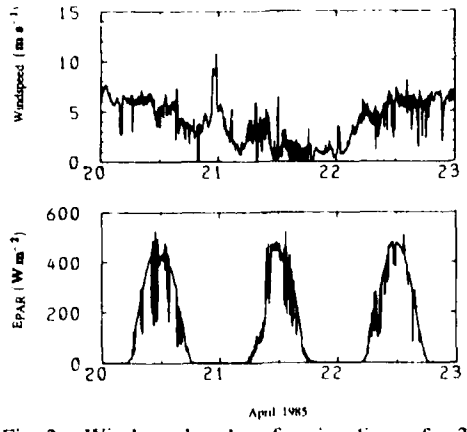

Fig. 2. Windspeed and surface irradiance for 20–22 April 1985.

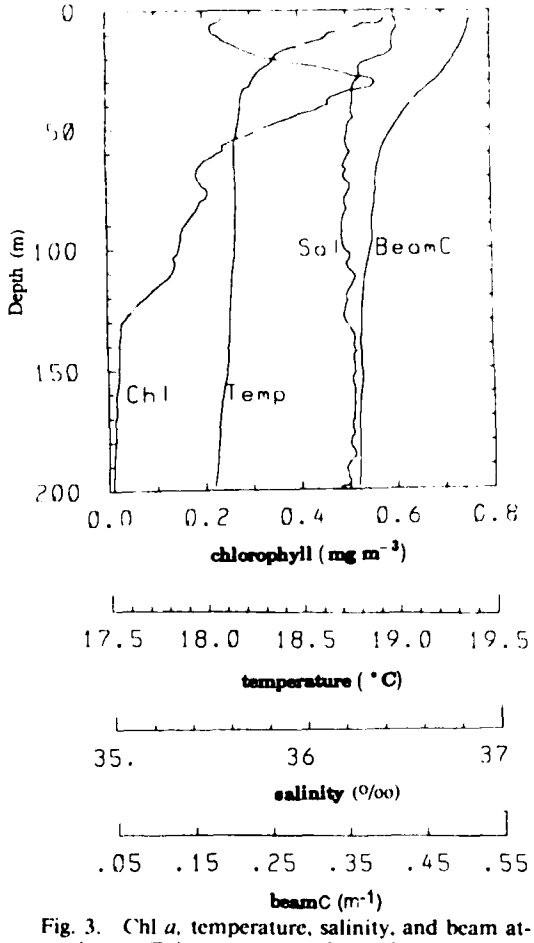

Fig. 3. Chl *a*, temperature, salinity, and beam attenuation coefficient at 660 nm for station-cast 19.51, 22 April 1985.

increasing trend through the time that station 19 was occupied.

Figure 3 shows the primary features of the water column characteristic of the time period. A subsurface chlorophyll maximum existed at 30–40 m, with a magnitude of about 0.6 mg m $^{-3}$. As in some other environments (Herbland and Voituriez 1979; Marra et al. 1987), the chlorophyll maximum coincided with the depth of the nitricline at 30–35 m. This structure is consistent with postbloom conditions where the stratified upper layer has been depleted of nutrients by biological activity. That is, the water-column characteristics suggest incipient stratification and surface warming, consistent with the data shown in Fig. 2, and depletion of nutrients near the surface. The depth of the euphotic zone (nominally defined as the depth of 1% of surface PAR) was at 70–80 m.

Absorption spectra—Absorption spectra for particulate matter, $a_p(\lambda)$, for cast 19.50 are shown in Fig. 4A. These spectra, obtained with a modified opal glass technique as described by Kiefer and SooHoo (1982) and Kishino et al. (1985), represent the total absorption by particles retained on a GF/F filter and include living phytoplankton with both photosynthetic and photoprotective pigments, fecal material, detrital pigments, bacteria, small heterotrophic protozoans, and other detritus. Optical means of separating detritus from other absorption in these spectra are only beginning to become established (Morel and Bricaud 1986; Cleveland et al. 1989; Bidigare et al. 1987; Iturriaga and Siegel 1988). Here, $a_p(\lambda)$ is determined by particles retained on glass-fiber filters measured with a scanning spectrophotometer. After this measurement, the filter paper was extracted with methanol and the decolorized filter paper was again measured to provide the spectral absorption coefficient of nonphotosynthetic particles, $a_{dc}(\lambda)$ (Fig. 4B). The absorption coefficient of particulate material, $a_p(\lambda)$, is taken as the sum of phytoplankton absorption, $a_{pl}(\lambda)$, and detrital absorption, $a_{dc}(\lambda)$,

$$a_p(\lambda) = a_{pl}(\lambda) + a_{dc}(\lambda). \qquad (12)$$

It has been assumed that absorption of inorganic particles is negligible. The derived phytoplankton spectrum is shown in Fig. 4C.

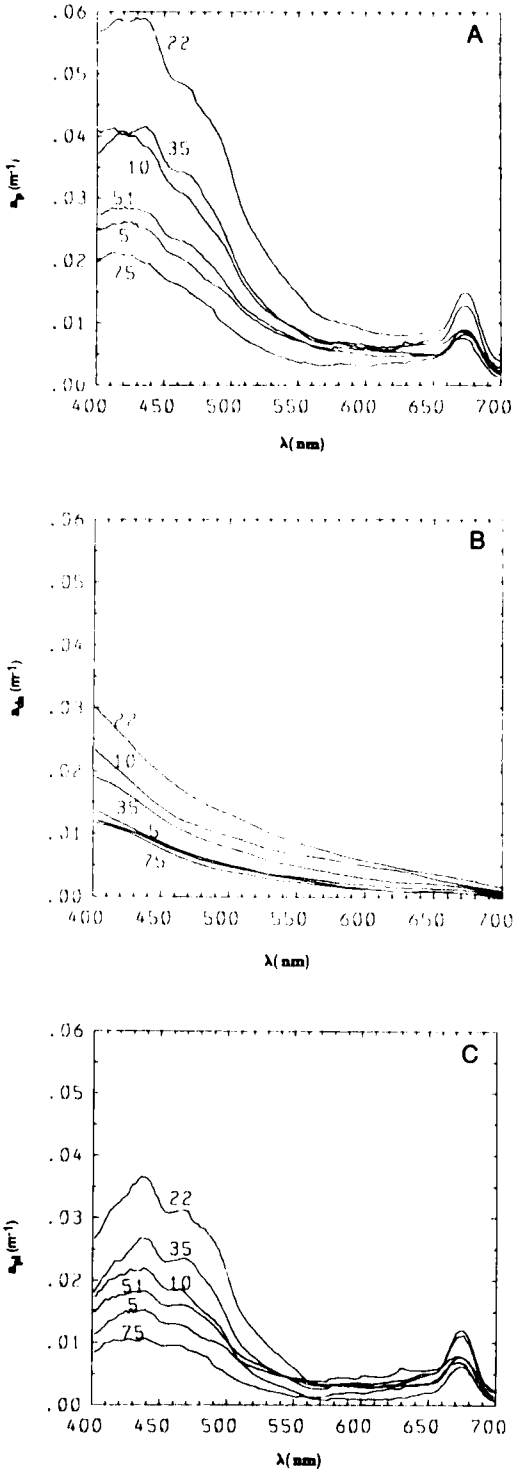

Fig. 4. Station-cast 19.50 for depths shown (m). A. The particle absorption spectra. B. The detritus spectra. C. The resultant phytoplankton spectra.

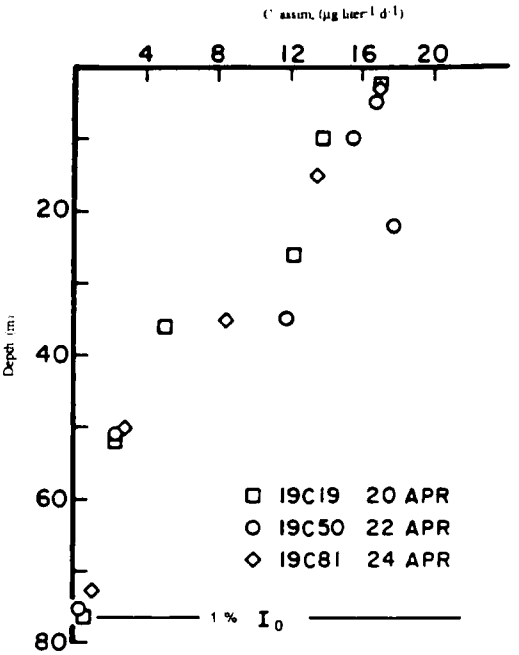

Fig. 5. Carbon assimilation from ^{14}C for three in situ experiments during the occupation of station 19.

Total absorption increases as a function of depth from 5 to 22 m and is correlated with increases in chlorophyll concentration. Chlorophyll-specific absorption of the detrital component is greatest at 10 m, which suggests a higher proportion of detritus to phytoplankton at this depth. Below 35 m, both the chlorophyll concentration and $a_p(\lambda)$ decrease with depth, suggesting that the concentration of nonphytoplankton-absorbing particles may be correlated with phytoplankton pigments. There is no indication of phycoerythrin in the spectra, which would appear as a peak or shoulder near 550 nm (Fig. 4A). The cyanobacteria at this station may have phycourobilin rather than phycoerythrin as their primary accessory pigment. Wavelength-averaged particle absorption is maximal at 22 m—a depth shallower than the chlorophyll maximum itself. This maximum corresponds with that in zeaxanthin and the cyanobacterial maxima.

Primary production—The rates of primary production (Fig. 5) are high for an open-ocean locale, but are not unexpected during spring in the Sargasso Sea (cf. Menzel and Ryther 1960). The areal rates average

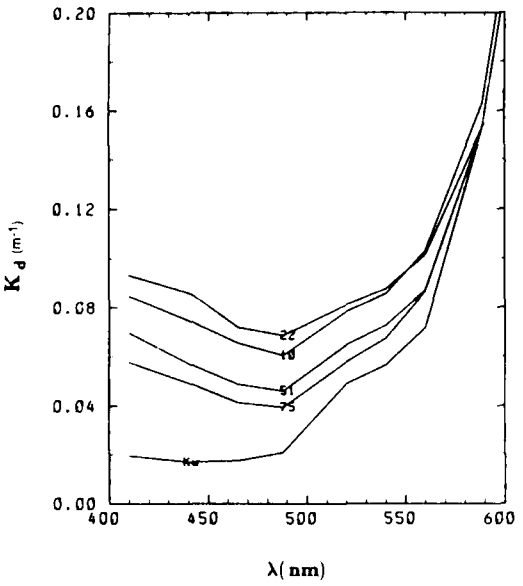

Fig. 6. Total spectral diffuse attenuation coefficient for 10, 22, 51, and 75 m at station-cast 19.51 and for clear water (K_w).

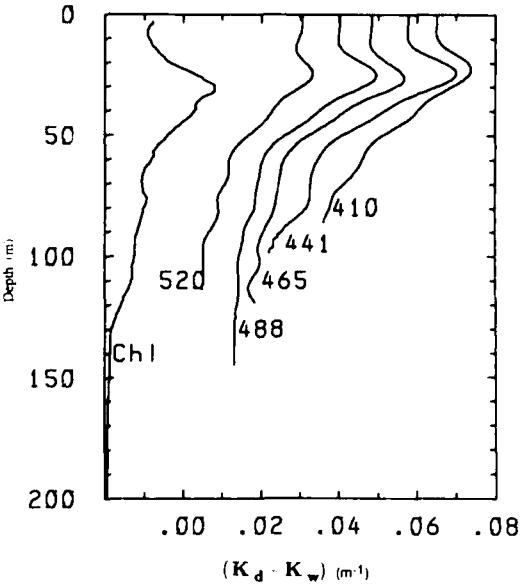

Fig. 7. Diffuse attenuation coefficients (station-cast 19.51) for the wavelengths (nm) shown after subtraction of the attenuation coefficient of pure seawater, $K_d(\lambda) - K_w(\lambda)$. Also shown is the chlorophyll profile for this cast.

about 500 mg C m^{-2} d^{-1}. Carbon assimilation averaged over all three experiments (20, 22, and 24 April) appears roughly constant through the upper 20 m and declines exponentially below that. The maximum on this profile at 22 m corresponds to the depth of maximum particle absorption shown in Fig. 4. Cyanobacteria and small eucaryotes (< 1-μm diam) are responsible for about 60% of the total primary production at this station (Iturriaga and Marra 1988).

Photosynthesis as a function of irradiance, P-I—The maximal photosynthetic rate normalized to chlorophyll concentration for station 19 averages 2.3 mg C (mg Chl *a*)$^{-1}$ h^{-1} and did not change with depth in the upper 100 m. The initial slope of the *P-I* curve (α)—an indication of the efficiency of photon capture at low irradiances—increases with depth from 0.01 mg C (mg Chl *a*)$^{-1}$ h^{-1} (μmoles photons m^{-2} s^{-1})$^{-1}$ at the surface to 0.025 at depth. The irradiance at which photosynthesis becomes light saturated, I_k, is another indication of photon capture efficiency at low irradiance. The ratio of light-saturated photosynthesis to α decreased with depth from a maximum >300 μmoles photons m^{-2} s^{-1} at the surface to 50 at 100 m, indicating that deeper living phytoplankton require less light to attain maximal rates of photosynthesis.

The quantum yield of photosynthesis is a more useful parameter in the context of a photon budget because it indicates the amount of photosynthetic carbon that is fixed relative to the photons absorbed. The maximum quantum yield is calculated with α from *P-I* measurements and particle absorption coefficients (Fig. 4). For station 19, the spectrally averaged maximal quantum yields based on only the phytoplankton component of absorption range from 0.041 to 0.075 moles C (moles photons absorbed)$^{-1}$.

Bio-optical properties—The bio-optical data are summarized in Figs. 6, 7, and 8. Figure 6 shows the wavelength dependence of diffuse attenuation for downwelling irradiance, $K_d(\lambda)$, at selected depths. These have been used for subsequent calculations of K_{PAR}. For wavelengths <580 nm, there is a depth dependence of $K_d(\lambda)$, with $K_d(\lambda)$ first increasing with depth until the depth of the particle and pigment maxima, and then declining with depth. The influence of total particle absorption on diffuse atten-

uation can be appreciated by comparing the relative changes with depth of particle absorption (Fig. 4A) and the total attenuation coefficient (Fig. 6). Consistent with the discussion leading to Eq. 10–12, the spectral shape of the diffuse attenuation coefficient is strongly influenced by the spectral shape of absorption from water, phytoplankton, detritus, and dissolved organic material. The strong increases in attenuation at ~500 and 590 nm coupled with increasing absorption in the blue (DOM), and phytoplankton and their by-products, produces a wavelength of maximum penetration between 480 and 490 nm.

Figure 7 shows the attenuation coefficients for five wavelengths of underwater light after removal of the attenuation coefficient for water. We use $K_w(z, \lambda)$ for clear natural waters as given by Smith and Baker (1981) and have estimated and accounted for change in the average cosine with depth. Figure 7 also shows the chlorophyll distribution as a function of depth as determined with the BOPS in situ fluorometer normalized with discrete chlorophyll samples. In addition to attenuation by water, which is largely a component converted to heat, Fig. 7 illustrates that chlorophyll and other phytoplankton pigments determine, in large degree, the distribution of the remaining light in the euphotic zone. Thus, most wavelengths in the visible region are affected by chlorophyll pigments and by the pigments which covary with chlorophyll. This point has been made previously by Smith and Baker (1978) and more recently by Siegel and Dickey (1987). The chlorophyll maximum is slightly deeper than the absorption maximum (note peaks in the $K_d - K_w$ profiles). The attenuation maximum corresponds with the particle attenuation maximum (Fig. 4A) and with the subsurface production maximum (Fig. 5).

In order to partition attenuation into components beyond the removal of that from water, we consider the measurements of particles and pigments. In analogy with Eq. 12, the attenuation by particles, $K_p(z)$, can be attributed to that from phytoplankton, $K_{pl}(z)$, plus that from detritus, $K_{de}(z)$:

$$K_p(z) = K_{pl}(z) + K_{de}(z). \quad (13)$$

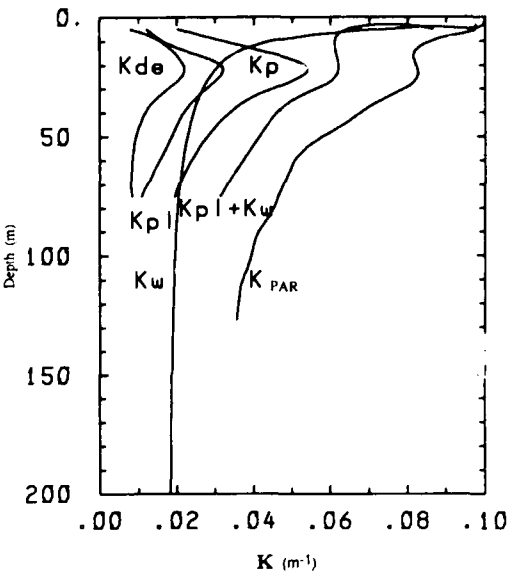

Fig. 8. Comparison of diffuse attenuation coefficients for pure seawater (K_w), phytoplankton (K_{pl}), detritus (K_{de}), and the total particle attenuation (K_p) with the total diffuse attenuation coefficient for PAR (K_{PAR}). The attenuation caused by the sum of detrital material and dissolved organic material is approximated by the difference between K_{PAR} and the sum of K_{pl} and K_w.

Following Eq. 8, the attenuation of particulate matter can be approximated by

$$K_p(z) = a_p'(z)/\bar{\mu}_d(z) + b_{bdp}^*(z) \quad (14a)$$

where $\bar{\mu}_d$ is the average cosine for downwelling irradiance, a_p' the absorption of particulate matter weighted by spectral irradiance at each depth, and b_{bdp}^* the diffuse backscattering coefficient for downwelling irradiance from particles. Using our direct observations of spectral reflectance, $R(z, \lambda)$, and the results of a Monte Carlo simulation (Kirk 1981), we estimate that $b/a \simeq 3$, $\bar{\mu}_d \simeq 0.8$, and $b_{bdp}^* \simeq 0.1 \times a_p'$ for these waters. Thus,

$$K_p(z) \approx 1.35 \times a_p'(z) \quad (14b)$$

where

$$a_p'(z) = \frac{\int a_p(z, \lambda) \times E_d(z, \lambda)\lambda \, d\lambda}{\int E_d(z, \lambda)\lambda \, d\lambda} \quad (15)$$

is the spectrally weighted particle absorption coefficient. In an analogous manner, if we know $a_{de}(z, \lambda)$ and $a_{pl}(z, \lambda)$, we can estimate $K_{de}(z, \lambda)$ and $K_{pl}(z, \lambda)$ with the above equations. Table 1 summarizes the spec-

Table 1. Biowatt '85 station-casts 19.50–19.51. Absorption with z (m) and a_i' (m^{-1}).

z	a_p'	a_{pl}'	a_{de}'	a_{pl}'/a_p'	a_{de}'/a_p'
5	0.0149	0.0090	0.0059	0.60	0.40
10	0.0237	0.0121	0.0116	0.51	0.44
22	0.0400	0.0238	0.0163	0.60	0.38
35	0.0281	0.0178	0.0103	0.63	0.36
51	0.0203	0.0135	0.0068	0.66	0.35
75	0.0144	0.0081	0.0063	0.56	0.47

trally weighted absorption coefficients and Table 2 the diffuse attenuation coefficients.

Figure 8 shows the result of partitioning the attenuation of PAR, $K_{PAR}(z)$, into several of its components. The (broadband) variability of K_w for PAR varies with depth, because as solar radiation penetrates to depth, those wavelengths where water absorbs most strongly (far blue and red) are rapidly reduced in their contribution to attenuation, whereas the wavelengths absorbed less strongly penetrate to greater depths. In addition, $\bar{\mu}_d$ varies slightly with depth. As a consequence, K_w(PAR) is relatively large near the surface and then approaches the value for the attenuation of the wavelength of maximum penetration, K_w (450 nm) = 0.017 m^{-1}, with increasing depth (Smith and Baker 1986). The effect on $K_{PAR}(z)$ is evident. The attenuation by detritus, K_{de}, and that by phytoplankton, K_{pl}, increase to maxima at ~22 m—the particle attenuation maximum (Fig. 4A, B) as well as the production maximum (*see Fig. 5*). At this depth, attenuation by other constituents is relatively small compared to shallower or deeper. The difference between K_{PAR} and the sum of K_w and K_{pl} represents the attenuation of dissolved plus detrital

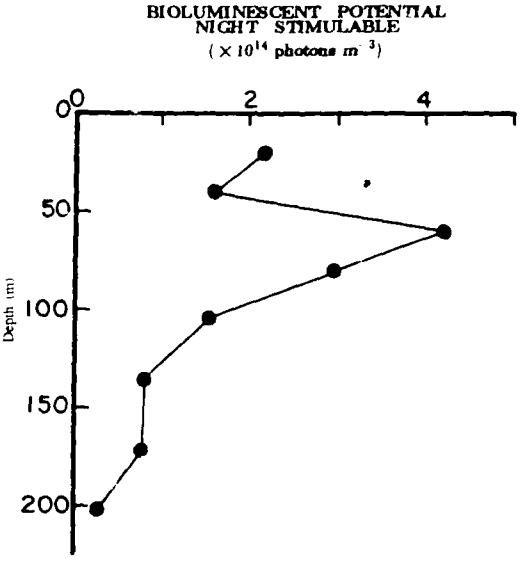

Fig. 9. The depth distribution of total stimulable bioluminescence (photons m^{-3}) measured with the bathyphotometer.

material in the water column. K_{PAR} decreases quickly near the surface, but assumes a nearly constant value over the depth range occupied by the chlorophyll maximum. However, maximum particle absorption, a_p', occurs at the top portion of the chlorophyll maximum. K_{PAR} approaches K_w, the attenuation of PAR for pure water by 200 m, which is roughly twice the depth of the euphotic zone. This partitioning of the attenuation of PAR provides a first-order assessment of the relative contribution to the attenuation of radiant energy by phytoplankton and its degradation products.

Bioluminescence properties—For the night MOCNESS tows (21 April, the depth of the 50% level of cumulative water-column biomass (displacement volume) was 43 m. For

Table 2. Biowatt '85 station-casts 19.50–19.51. Attenuation with z (m) and K_i (m^{-1}).

z	K_{PAR}	K_w	K_p	K_{pl}	K_{de}	K_γ	$K_{de+\gamma}$	$\frac{K_{de}}{K_{pl}}$	$\frac{K_w}{K_{PAR}}$	$\frac{K_p}{K_{PAR}}$	$\frac{K_{pl}}{K_{PAR}}$	$\frac{K_{de}}{K_{PAR}}$	$\frac{K_\gamma}{K_{PAR}}$	$\frac{K_{de+\gamma}}{K_{PAR}}$
5	0.098	0.074	0.020	0.012	0.008	0.004	0.012	0.67	0.76	0.20	0.12	0.08	0.04	0.12
10	0.086	0.045	0.032	0.016	0.016	0.009	0.025	1.00	0.52	0.37	0.19	0.19	0.10	0.29
22	0.083	0.030	0.054	0.032	0.022	−0.001	0.021	0.69	0.36	0.65	0.39	0.27	−0.01	0.25
35	0.073	0.026	0.038	0.024	0.014	0.009	0.023	0.58	0.35	0.52	0.33	0.19	0.12	0.31
51	0.057	0.023	0.027	0.018	0.009	0.007	0.016	0.50	0.40	0.47	0.32	0.16	0.12	0.28
75	0.046	0.021	0.019	0.010	0.009	0.006	0.015	0.90	0.46	0.41	0.22	0.20	0.13	0.33

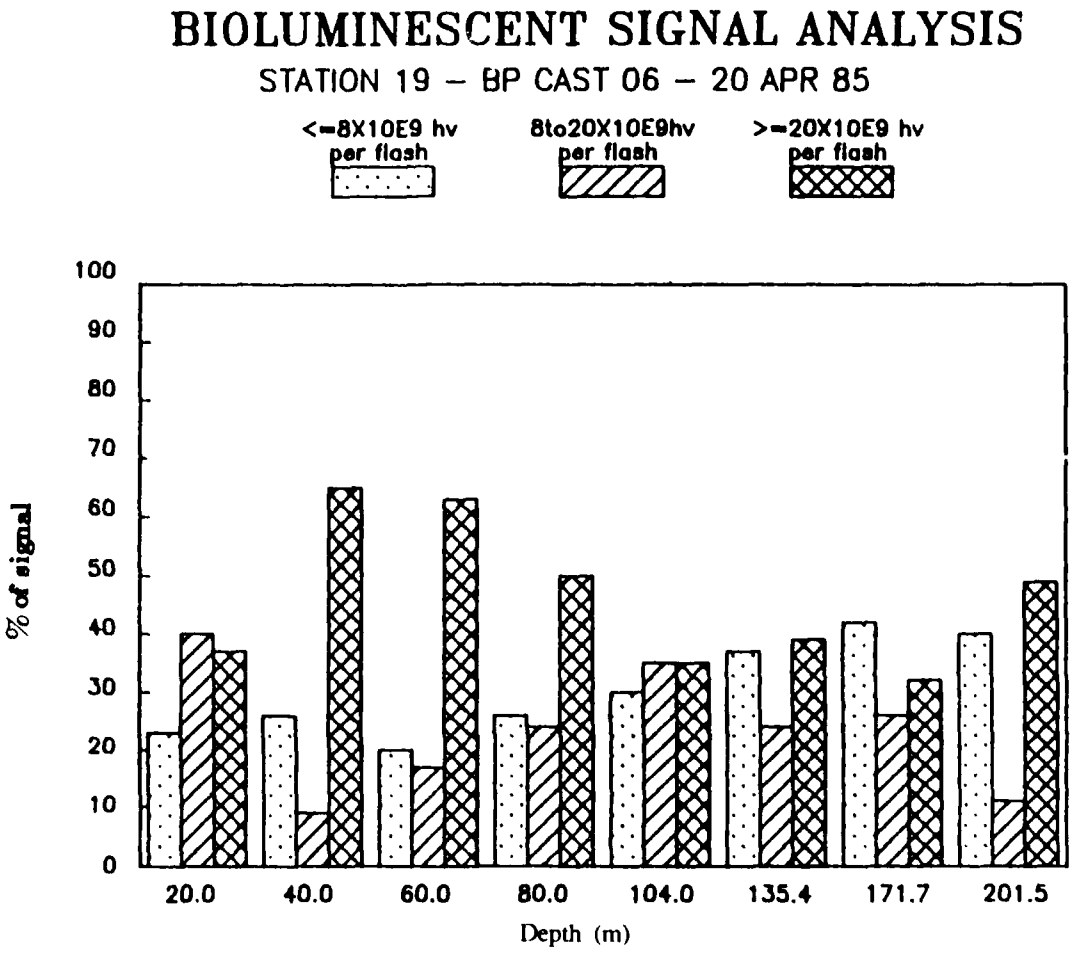

Fig. 10. Distribution of bioluminescent flash intensity as a function of depth.

the day MOCNESS tow (22 April), this depth was 93 m. This difference suggests considerable vertical migration of zooplankton biomass within the upper 800 m. The total cumulative water-column biomass for the upper 800 m is 36% greater for the night than for the day tows, suggesting net avoidance during day tows.

The profile of bioluminescence potential for station 19 is shown in Fig. 9. Bioluminescence potential—the total amount of stimulable bioluminescence per unit volume—has been calculated as 10 times the bioluminescence light measured by the bathyphotometer because only about a tenth of the light of the bioluminescence potential of the dinoflagellate *P. noctiluca* is detected when it passes through our bathyphotometer (Swift et al. 1985). Here we have assumed that other organisms behave similarly. In agreement with this assumption, *Pleuromamma* species have recently been shown to release about 15% of their bioluminescence potential when passing through the bathyphotometer (H. Batchelder pers. comm.).

The observed flashes were separated into three energy categories (<8, 8–20, and >20 $\times 10^9$ photons per flash) in order to determine their biological source. Figure 10 shows the results of this analysis as a function of depth in the profile of bioluminescence potential shown in Fig. 9. The bioluminescence in the peak between 40 and 80 m was

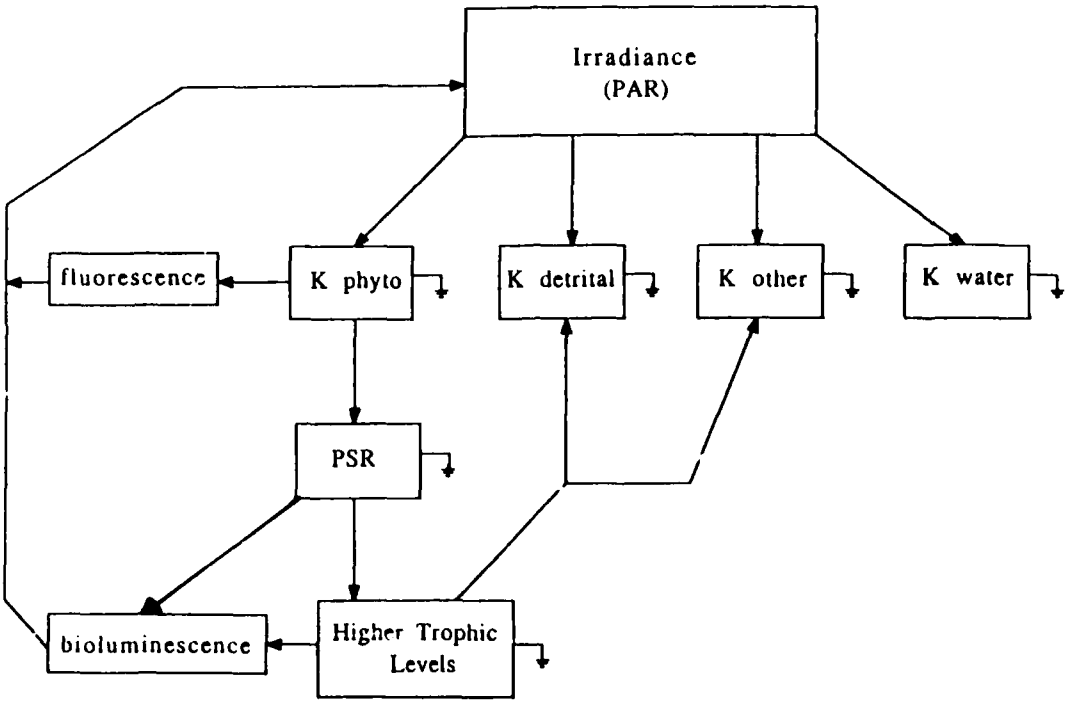

Fig. 11. Schematic of the photon budget.

produced primarily by large organisms producing flashes of $>20 \times 10^9$ photons. Outside this depth range, no group showed a marked dominance in the production of stimulated bioluminescence.

Discussion

General—Figure 11 describes the scheme used to summarize the bio-optical data into a photon budget, with irradiance at each depth attenuated by various absorption and scattering avenues and increased slightly by fluorescence and bioluminescence. According to Duntley (1963), the net absorption of radiant energy, Q (expressed as quanta), in any element of volume dV in any horizontal lamina of thickness dz at depth z can be approximated by

$$\frac{dQ}{dV} = -\frac{dE_{qPAR}}{dz}, \tag{16}$$

where dQ/dV is the number of photosynthetically available quanta absorbed per unit volume and E_{qPAR} is the quantum irradiance for PAR. By definition the total diffuse attenuation coefficient for PAR is given by

$$K_{qPAR} = \frac{-1}{E_{qPAR}} \times \frac{dE_{qPAR}}{dz}, \tag{17}$$

so the absorbed quantum flux per volume is

$$\frac{dQ}{dV} = E_{qPAR} \times K_{qPAR}. \tag{18}$$

For this open-ocean station, the ratio of scattering to absorption is relatively small, so the total attenuation coefficient can be approximately partitioned into a set of partial attenuation coefficients as described earlier. The complete photon budget for PAR, including source terms, can be written

$$E_{qPAR}(z) = E_{qPAR}(0^-) \exp\left[-\int_0^z K_{qPAR}(z) \times dz\right] + Fl(z) + Bl(z) \tag{19}$$

where $Fl(z)$ and $Bl(z)$ are the fluorescence and bioluminescence, respectively, at depth z. In this discussion we assume that processes of transpectral scattering (Preisendorfer and Mobley 1988; Marshall and

Smith 1990), e.g. Raman and Brillouin, are negligible and treat fluorescence and bioluminescence as source terms in their respective wavelength bands. Then,

$$\frac{dE_{qPAR}}{dz} = -E_{qPAR}(z)K_w(z) - E_{qPAR}(z)K_p(z) - E_{qPAR}(z)K_y(z) + \frac{dFl}{dz} + \frac{dBl}{dz}. \quad (20)$$

As noted above, we have carried out all the computations for broadband PAR as a function of wavelength so that all spectral variability, possible nonlinearities, and sensitivity have been retained and accounted for. Values of $E_d(z, \lambda)$ are determined from the BOPS data, and E_{qPAR} and K_{qPAR} are then computed from these as described in the methods section. The data for the photon budget are plotted on a log-linear scale in Fig. 12. The total daily photosynthetically available radiant energy, E_{qPAR}, incident above the surface and integrated over the daylight period (22 April 1985) during this study equals 53.3 moles photons m^{-2} d^{-1}.

Note that this computation of daily $E_{qPAR}(z)$ does not explicitly include vertical mixing, horizontal variations, organism motility, or sinking. A further qualification regarding the photon budget as presented here includes the knowledge that $b/a \approx 3$ throughout most of the water column, except in the particle maximum where this ratio increases to ~5. The increased scattering at the depth of the particle maxima decreases the accuracy of computations based on partitioning of the attenuation coefficient, especially when computing the difference between nearly equal components. It is apparent in the estimate of the dissolved organic material component, K_y, at 22 m where the derived value is smaller than the estimated error in the K-values, which is roughly ± 0.005 m^{-1}.

Attenuation of PAR—The product of the quantities $E_{PAR}(z)$ and K_{qPAR} (Eq. 18) provides an estimate of the daily total quanta absorbed per unit volume as a function of depth. This estimate includes attenuation of PAR by all dissolved and suspended constituents as is summarized in Table 3. The

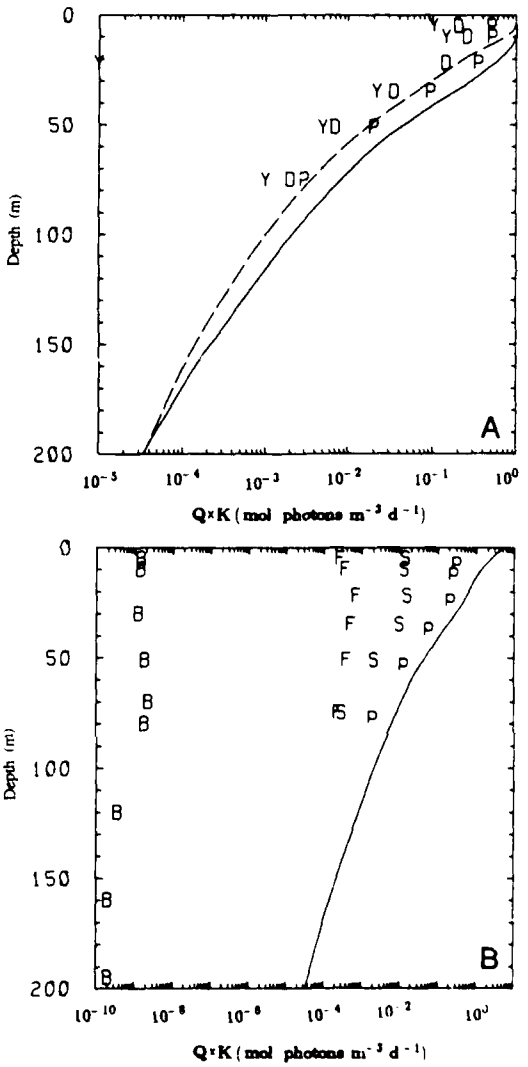

Fig. 12. A. Distribution of photons (photons m^{-1}) as a function of depth emphasizing: components of total photons ($Q_{PAR} \times K_{PAR}$—solid line); photons lost to absorption of water ($Q_{PAR} \times K_w$—dashed line); photons lost to total particle absorption ($Q_{PAR} \times K_p$—P); photons lost to detrital material absorption ($Q_{PAR} \times K_d$—D); photons lost to dissolved organic material absorption ($Q_{PAR} \times K_y$—Y). B. Distribution of photons (photons m^{-1}) as a function of depth partitioned into various components: total photons ($Q_{PAR} \times K_{PAR}$—solid line); photons lost to absorption of phytoplankton ($Q_{PAR} \times K_{ph}$—p); photosynthetically stored radiation (PSR—S); fluorescence (F); bioluminescence (B).

percentage contribution by each component is summarized in Table 2. The attenuation caused by viable phytoplankton, K_{ph}/K_{PAR}, is relatively high for open-ocean waters (e.g.

Table 3. Biowatt '85 station-casts 19.50–19.51 with z (m), Q_{PAR} (moles photons m^{-3} d^{-1}), $Q \times K_t$ (moles photons m^{-3} d^{-1}), and PSR (moles photons m^{-3} d^{-1}).

z	Q_{PAR}	$Q \times K_{PAR}$	$Q \times K_c$	$Q \times K_p$	$Q \times K_w$	$Q \times K_{dr}$	$Q \times K_y$	$Q \times K_{dr+y}$	PSR
0	53.290								
5	25.679	2.517	1.900	0.514	0.308	0.205	0.103	0.308	0.0140
10	16.161	1.390	0.727	0.517	0.259	0.259	0.145	0.404	0.0129
22	6.628	0.550	0.199	0.358	0.212	0.146	−0.007	0.139	0.0153
35	2.488	0.182	0.065	0.095	0.060	0.035	0.022	0.057	0.0099
51	0.743	0.042	0.017	0.020	0.013	0.007	0.005	0.012	0.0021
75	0.176	0.008	0.004	0.003	0.002	0.002	0.001	0.003	0.0003

Kirk 1983, table 10.2) and suggests an increased effectiveness in the utilization of radiant energy during postbloom conditions. At depths below the major contribution of phytoplankton (i.e. below the depth of the chlorophyll maximum), total attenuation approaches that caused by water alone.

Attenuation by particulates is estimated by multiplying $E_{qPAR}(z)$ by $K_p(z)$, where $K_p(z)$ was derived from directly measured particulate absorption spectra as described above (Fig. 4A). Maximum absorption occurred at 22 m, above the chlorophyll maximum, and within the surface production maximum. In general, the attenuation by particles shows broad maxima at middepths in the euphotic zone, consistent with the distribution of chlorophyll.

In contrast, the depth distribution of the total beam attenuation coefficient (Fig. 3) at 660 nm, c(660 nm), shows a gradual increase from below the euphotic zone to the surface. Since particle absorption at 660 nm is relatively small, this variation in c(660 nm) is primarily caused by particle scattering and thus is a proxy measure of particle volume concentration if particle size distribution and index of refraction remain relatively constant (Jerlov 1976). For the data considered here, c(660 nm) and total particle volume computed as the sum of all particle volumes with spherical diameters of 2–25 μm are highly correlated. Thus, c(660 nm) is an independent optical indicator of particle number volume. The decrease in particle volume, as inferred from beam transmittance and Coulter counter data, and the increase in particle absorption with depth provide strong evidence that absorption per cell volume is increasing with depth. That is, these data are consistent with the hypothesis of near-surface photoadaptation and an increase in pigment concentration per cell volume with increasing depth. Both processes serve to optimize the utilization of radiant energy by phytoplankton.

That fraction of radiant energy absorbed by the phytoplankton, or PUR (Morel 1978), can be estimated by $E_{qPAR}(z) \times K_{pl}(z)$. Absorption by particulate detrital material is determined by the difference between the total and phytoplankton absorption. The depth variability of these quantities shows that it is attenuation by biogeneous material that provides the optical variability in these waters.

Knowledge of the absorption from total particulate material allows the dissolved component to be estimated by the difference,

$$K_y(z) = K_{qPAR}(z) - [K_p(z) + K_w(z)]. \quad (21)$$

In this application, K_y is most likely dissolved organic matter because the method of determining phytoplankton absorption (Figs. 4, 8) will include other particulate components. As mentioned above, the apparent minimum in the attenuation by DOM at the same depth of the attenuation maximum for phytoplankton (22 m) may be because of the relatively greater particulate material at this depth and/or a consequence of the decreased accuracy of the partitioning of the attenuation coefficient at the depth of maximum b/a ratio. Clearly, more work is required to estimate K_y independently and with increased accuracy.

The spectrally weighted absorption, determined with greater precision than the attenuation coefficient, shows that the relative absorption of the phytoplankton compo-

Table 4. Biowatt '85 station-cast 19.50. Pigments with z (m) and concentrations (ng/liter $^{-1}$) of chlorophyllide *a*, chlorophyll *c*, peridinin, fucoxanthin, 19'-hexanoyloxyfucoxanthin, prasinoxanthin, diadinoxanthin, zeaxanthin, chlorophyll *b*, chlorophyll *a*, and carotene.

z	Chl-ide *a*	Chl *c*	Per.	Fucox.	H-fucox.	Pras.	Diad.	Zea.	Chl *b*	Chl *a*	Carot.
5	0	26	0	19	71	0	22	30	29	189	0
10	11	38	7	45	71	8	41	35	64	217	0
22	0	46	8	74	105	29	8	50	139	421	7
35	0	97	0	86	129	27	18	13	171	462	5
51	39	37	0	74	95	10	41	12	67	317	0
75	10	27	0	80	90	5	35	0	63	237	0

nent to the total particle absorption is nearly uniform throughout the euphotic zone (Table 1). This is true even though the phytoplankton assemblages and corresponding pigment concentrations suggest a layered distribution with depth (Bidigare et al. 1989). Bidigare et al. (1989) showed that the cyanobacteria, dinoflagellates, golden-brown algae (diatoms and/or chrysophytes), and green algae (including the prasinophytes) occur at increasingly greater depths in layers with the phytoplankton composition shifting from a golden-brown-dominated community at 5 m to a green-dominated community at 44 m. Table 4 gives the concentrations (in ng) of the pigment concentrations observed at station 19.50 which are representative of the pigment distribution for this photon budget. Coccoid cyanobacteria (Iturriaga and Marra 1988) and the relative concentration of zeaxanthin (plus lutein) to Chl *a* have their highest concentrations in the upper 20–30 m. Prasinoxanthin, a pigment marker for cyanobacteria, shows both a maximum concentration and a maximum relative to Chl *a*, which is an indicator of the relative importance with respect to total pigment biomass, at the depth of the absorption maximum of 22 m. These pigment data indicate that prasinophytes and cyanobacteria are major contributors within the absorption maximum. Fucoxanthin, 19'-hexanoyloxyfucoxanthin, and Chl *b* all show a maximum corresponding to the Chl *a* maximum at 35 m, indicating that prymnesiophytes and Chl *b*-containing algae are major contributors at the depth of the Chl *a* maximum. This layering of phytoplankton assemblages is consistent with the hypothesis that organisms with pigment composition most nearly matched to the spectral irradiance at a given depth will have a performance edge and will become dominant at that depth. These combined optical and pigment data suggest phytoplankton assemblages arranged as a function of depth in a way that is remarkably effective in maintaining a relatively uniform absorption of photons throughout the euphotic zone.

Photosynthetically stored radiation (PSR)—A fraction of the photons absorbed by phytoplankton effect the photosynthetic conversion of carbon. This fraction is photosynthetically stored radiation (PSR) which is the irradiance equivalent of carbon assimilation. The minimum number of photons required to produce PSR can be computed from the minimal quantum requirement of 10 moles of photons needed to reduce 1 mole of carbon (Kok 1960). For 22 April (station-cast 19.50), PSR was determined from 12-h in situ carbon assimilation measurements to be 0.0610 moles of reduced C m^{-2}, equivalent to 0.61 moles photons m^{-2}. This value is an underestimate of the photon-to-carbon conversion to the extent that the ^{14}C method for measuring primary production cannot account for autotrophic respiration. PSR averaged 1.2% of the total PAR quanta available on 22 April—a value indicative of a relatively effective utilization of energy for oceanic waters.

There is a slight maximum in PSR values (Table 3) at 22 m which coincides with a maximum in absorption. However, the PSR maximum may not be significant. At depths >30 m the quantum yield of photosynthesis approached maximal values. This trend is also evident in the slope of the PSR profile in Fig. 13. The consistency of the PSR results (i.e. comparison of the carbon assimilation derived component to the directly

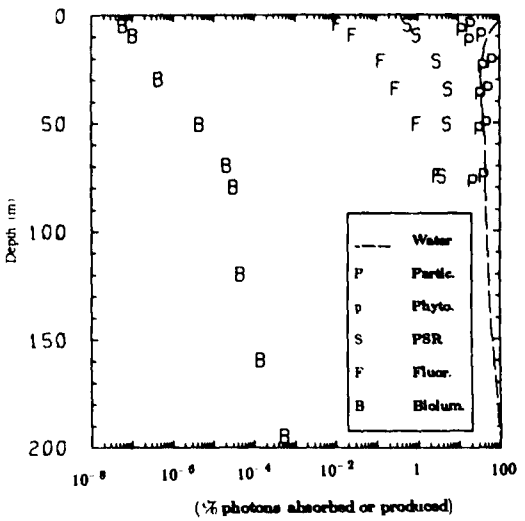

Fig. 13. Percentage of available quanta absorbed or produced, for various components, as a function of depth.

determined irradiance component) is an indication of close, but not exact, closure of the photon budget.

Fluorescence—An additional and smaller fraction of photons absorbed by phytoplankton are not channeled into photosynthesis but rather are re-emitted as red fluorescent photons. Although the upwelled fluorescence signal in the ocean is small, that caused by chlorophyll at 683 nm is detectable (Topliss 1985) and has been interpreted in terms of photosynthesis (Topliss and Platt 1986; Kiefer et al. 1989). The quantitative relationship among absorption, photosynthesis, and fluorescence is presently controversial even in laboratory studies and merits further study. Although we have determined the natural fluorescence at 683 nm, we do not have full spectral information. We have assumed that fluorescence is a constant 3% of absorbed photons (Latimer et al. 1956; Falkowski and Kiefer 1985) and ignore possible influences of inelastic scattering (Marshall and Smith 1990) on algal photobiology.

Bioluminescence—Because we do not have measurements of herbivore grazing or carnivorous activity, we cannot estimate the amount of PSR energy passed to zooplankton. Similarly, we cannot estimate the amount of fixed carbon passing to microheterotrophs such as bacteria. Thus, we lack the data to establish mechanistic linkages between optical and bioluminescence variability. However, phytoplankton biomass (measured as Chl *a*) did not change appreciably for the 2-d period before 22 April, the day chosen to construct the photon budget. Therefore, if production and consumption are in rough balance, sinking and mixing taken to be small, and assuming a 50% assimilation efficiency, we can estimate a transfer of 50% of the PSR.

From the zooplankton distribution data (E. Swift pers. comm.) and from our knowledge of the distribution and intensities of bioluminescence, the amount of bioluminescent light produced for the budget is calculated. As described above, this calculation assumes that the biological efficiency of the bathyphotometer is 10%. Bioluminescence potential is analogous to a standing crop measurement, but unlike the other irradiances reported, it is not a flux. In order to make it comparable to the irradiances, we need to know the natural rates of bioluminescence, or we must estimate the rate at which organisms recover their bioluminescence potential after a flash. In the absence of knowledge of natural rates of bioluminescence, we estimate here that the recovery rate of bioluminescence potential is ~1 d to allow us to express bioluminescence as a photo flux. Measurements of the intensity of natural bioluminescence and measurements of recovery rates are necessary to refine future studies in this regard.

Features of vertical structure in the epipelagic community of bioluminescent organisms can be revealed by measuring the bioluminescence potential. The marked peak (nocturnal) in stimulated bioluminescence (Fig. 9) is about 20 m deeper than the depth of the subsurface chlorophyll maximum (Fig. 3). Signal analysis with data from Swift et al. (1985) for the amount of light produced by zooplankton suggests that the organisms producing most of the bioluminescence in the peak are copepods, larvaceans, and ostracods. Swift et al. (1985) previously reported high numbers of ostracods and larvaceans associated with sub-

surface peaks of stimulated bioluminescence in the northern Sargasso Sea in August. The samples for the data shown in Figs. 9 and 10 also contain high numbers of larvaceans and ostracods and small numbers of bioluminescent copepods. The formation of sharp subsurface peaks in stimulable bioluminescence by larvaceans and ostracods may be a general phenomenon in the northern part of the Sargasso Sea. For example, Ortner et al. (1980) reported a population maximum at 75–100 m in this region for larvaceans from MOCNESS samples taken in November and May. It may also indicate a preferential layering of zooplankton in response to the observed layering of phytoplankton. If so, there is the possibility that there are mechanistic and predictable linkages between these physical, chemical, and optical distributions and the bioluminescence. We were unable to establish such a linkage with the data reported here, presumably because of the complex trophic structure linking phytoplankton and bioluminescent zooplankton.

Photon budget—Because the log-linear scale (Fig. 12) obscures some of the fine-scale relationships of the budget, we have recast these data in Fig. 13 as the percentage of available quanta absorbed or produced at a particular depth. The range in photon flux within the budget spans about 10 orders of magnitude (Fig. 13). Most of the absorption of quanta is by water. Particulate material of biological origin is responsible for the remaining attenuation and the optical variability. Phytoplankton assemblages with varying pigment concentrations and growth rates (Table 4; Bidigare et al. 1989) are arranged as a function of depth in a way that is remarkably effective in maintaining a relatively uniform absorption of photons throughout the euphotic zone. Fluorescence and bioluminescence as sources of radiant energy are considerably smaller than photon sinks.

The photon budget as presented is preliminary. In part, this is because the source terms of bioluminescence and fluorescence have not previously been studied from a total energy budget perspective. Consequently, we have only rudimentary knowledge of the light production terms in contrast to the attenuation terms. This preliminary budget helps to identify and describe the biological absorbers, scatterers and producers of light within a defined physical, chemical, and optical environment. We have not dealt with the problem of radiative transfer of fluorescence or bioluminescence to parameterize the amount of light from these sources which might exit the ocean's surface. Our results show that the inclusion of grazing losses or other energy transfers to secondary producers is essential for full closure of the budget. In spite of the limitations of the data presented here, we argue that the photon budget will be an extremely useful construct for the study of oceanic optics and biology. It will be an important tool for the study of ocean ecosystems and particularly useful for investigating the possibility of mechanistic and predictable linkages between the attenuation (phytoplankton) and production (bioluminescence) terms. An accurate photon budget is a first step toward the prediction of production, biological behavior, and trophic structure from optical variables that are more easily and rapidly measured.

References

BAKER, K. S., AND R. FROUIN. 1987. Relation between photosynthetically available radiation and total insolation at the ocean surface under clear skies. Limnol. Oceanogr. **32**: 1370–1377.

———, AND R. C. SMITH. 1982. Bio-optical classification and model of natural waters. Limnol. Oceanogr. **27**: 500–509.

BARTZ, R., J. R. V. ZANEVELD, AND H. PAK. 1978. A transmissometer for profiling and moored observations in water, p. 102–108. *In* Ocean Optics 5, Proc. SPIE **160**.

BEERS, J. R. 1976. Determination of zooplankton biomass, p. 35–84. *In* H. F. Steedman [ed.], Zooplankton fixation and preservation. UNESCO.

BIDIGARE, R. R., J. H. MORROW, AND D. A. KIEFER. 1989. Derivative analysis of spectral absorption by photosynthetic pigments in the western Sargasso Sea. J. Mar. Res. **47**: 323–341.

———, R. C. SMITH, K. S. BAKER, AND J. MARRA. 1987. Oceanic primary production estimates from measurements of spectral irradiance and pigment concentrations. Global Biogeochem. Cycles **1**: 171–186.

CLEVELAND, J. S., M. J. PERRY, D. A. KIEFER, AND M. C. TALBOT. 1989. Maximal quantum yield of

photosynthesis in the northwestern Sargasso Sea. J. Mar. Res. In press.

DUNTLEY, S. Q. 1963. Light in the sea. J. Opt. Soc. Am. **53**: 214–233.

FALKOWSKI, P., AND D. A. KIEFER. 1985. Chlorophyll *a* fluorescence in phytoplankton: Relationship to photosynthesis and biomass. J. Plankton Res. **7**: 715–731.

FITZWATER, S. E., G. A. KNAUER, AND J. H. MARTIN. 1982. Metal contamination and its effect on primary production measurements. Limnol. Oceanogr. **27**: 544–551.

HERBLAND, A., AND B. VOITURIEZ. 1979. Hydrological structure analysis for estimating the primary production in the tropical Atlantic Ocean. J. Mar. Res. **37**: 87–101.

HERRING, P. J. [ED.]. 1978. Bioluminescence in action. Academic.

HØJERSLEV, N. K. 1974. Daylight measurements for photosynthetic studies in the western Mediterranean. Univ. Copenhagen Inst. Phys. Oceanogr. Rep. 26.

ITURRIAGA, R., AND J. MARRA. 1988. Temporal and spatial variability of chrococcoid cyanobacteria (*Synecchococcus* spp.): Specific growth rates and contribution to primary production in the Sargasso Sea. Mar. Ecol. Prog. Ser. **44**: 175–181.

———, AND D. SIEGEL. 1988. Microphotometric distinction of phytoplankton and detrital absorption properties, p. 277–287. *In* Ocean Optics 9, Proc. SPIE **924**.

JEFFREY, S. W., AND G. F. HUMPHREY. 1975. New spectrophotometric equations for determining chlorophylls *a*, *b*, c_1, and c_2 in higher plants, algae and natural phytoplankton. Biochem. Physiol. Pflanzen **167**: 191–194.

JERLOV, N. G. 1976. Marine optics, 2nd ed. Elsevier.

KIEFER, D. A., W. S. CHAMBERLIN, AND C. R. BOOTH. 1989. Natural fluorescence of chlorophyll *a*: Relationship to photosynthesis and chlorophyll concentration in the western South Pacific gyre. Limnol. Oceanogr. **34**: 868–881.

———, AND J. B. SOOHOO. 1982. Spectral absorption by marine particles. Limnol. Oceanogr. **27**: 492–499.

KIRK, J. T. O. 1981. Monte Carlo study of the nature of the underwater light field in, and the relationships between optical properties of, turbid yellow waters. Aust. J. Mar. Freshwater Res. **32**: 517–532.

———. 1983. Light and photosynthesis in aquatic ecosystems. Cambridge.

KISHINO, M., M. TAKAHASHI, N. OKAMI, AND S. ICHIMURA. 1985. Estimation of the spectral absorption coefficients of phytoplankton in the sea. Bull. Mar. Sci. **37**: 634–642.

KOK, B. 1960. Efficiency of photosynthesis, p. 566–633. *In* Encyclopedia of photosynthesis. V. 5. Springer.

LATIMER, P., T. T. BANNISTER, AND E. I. RABINOWITCH. 1956. Quantum yields of fluorescence of plant pigments. Science **124**: 585–586.

MARRA, J., AND E. O. HARTWIG. 1984. Biowatt: A study of bioluminescence and optical variability in the sea. Eos **65**: 732–733.

———, P. H. WIEBE, J. K. B. BISHOP, AND J. C. STEPIEN. 1987. Primary production and grazing in the plankton of the Panama Bight. Bull. Mar. Sci. **40**: 255–270.

MARSHALL, B. R., AND R. C. SMITH. 1990. Raman scattering and in-water ocean optical properties. Appl. Opt. **29**: 71–84.

MENZEL, D. W., AND J. H. RYTHER. 1960. The annual cycle of primary production in the Sargasso Sea off Bermuda. Deep-Sea Res. **6**: 351–367.

MITCHELL, B. G., AND D. A. KIEFER. 1988. Chlorophyll *a* specific absorption and fluorescence excitation spectra for light-limited phytoplankton. Deep-Sea Res. **35**: 639–663.

MOREL, A. 1978. Available, usable and stored radiant energy in relation to marine photosynthesis. Deep-Sea Res. **25**: 673–688.

———, AND A. BRICAUD. 1986. Inherent optical properties of algal cells including picoplankton: Theoretical and experimental results, p. 521–559. *In* Photosynthetic picoplankton. Can. Bull. Fish. Aquat. Sci. 214.

ORTNER, P. B., P. H. WIEBE, AND J. L. COX. 1980. Relationships between oceanic epizooplankton distributions and the seasonal deep chlorophyll maximum in the northwestern Atlantic Ocean. J. Mar. Res. **38**: 507–531.

PREISENDORFER, R. W. 1961. Application of radiative transfer theory to light measurements. Int. Union Geol. Geophys. Monogr. 10, p. 11–30.

———. 1976. Hydrologic optics. 6 V. NTIS, Springfield, VA.

———, AND C. D. MOBLEY. 1988. Theory of fluorescent irradiance fields in natural waters. J. Geophys. Res. **93**: 10,831–10,856.

SIEGEL, D. A., AND T. D. DICKEY. 1987. Observations of the vertical structure of the diffuse attenuation coefficient spectrum. Deep-Sea Res. **43**: 547–563.

SMITH, R. C., AND K. S. BAKER. 1978. Optical classification of natural waters. Limnol. Oceanogr. **23**: 260–267.

———, AND ———. 1981. Optical properties of the clearest natural waters (200–800 nm). Appl. Opt. **20**: 177–184.

———, AND ———. 1984. The analysis of ocean optical data, p. 119–126. *In* Ocean Optics 7, Proc. SPIE **489**.

———, AND ———. 1986. The analysis of ocean optical data, 2, p. 95–107. *In* Ocean Optics 8, Proc. SPIE **637**.

———, ———, AND P. DUSTAN. 1981. Fluorometric techniques for the measurement of oceanic chlorophyll in the support of remote sensing. Scripps Inst. Oceanogr. SIO Ref. 81-17.

———, C. R. BOOTH, AND J. L. STAR. 1984. Oceanographic bio-optical profiling system. Appl. Opt. **23**: 2791–2797.

SWIFT, E., W. H. BIGGLEY, AND E. J. LESSARD. 1985. Distributions of epipelagic bioluminescence in the Sargasso and Caribbean Seas, p. 235–258. *In* A. Zirino [ed.], Mapping strategies in chemical oceanography. Am. Chem. Soc.

TALBOT, M. C., D. S. THORESON, AND M. J. PERRY. 1985. Photosynthesis vs. light intensity measurements: A miniaturized incubator. Univ. Wash. School Oceanogr. Tech. Rep. 406.

TALLING, J. F. 1982. Utilization of solar radiation by phytoplankton, p. 619–631. *In* C. Helene et al. [eds.], Trends in photobiology. Plenum.

TOPLISS, B. J. 1985. Optical measurements in the Sargasso Sea: Solar stimulated chlorophyll fluorescence. Oceanol. Acta **8**: 263–270.

———, AND T. PLATT. 1986. Passive fluorescence and photosynthesis in the ocean: Implications for remote sensing. Deep-Sea Res. **33**: 849–864

WIEBE, P. H., K. H. BURT, S. H. BOYD, AND A. W. MORTON. 1976. A multiple opening/closing net and environmental sensing system for sampling zooplankton. J. Mar. Res. **34**: 313–326.

———, AND OTHERS. 1985. New developments in the MOCNESS, an apparatus for sampling zooplankton and micronekton. Mar. Biol. **87**: 313–323.